

1 Differential photosynthetic responses of marine planktonic and  
2 benthic diatoms to ultraviolet radiation under various temperature  
3 regimes

4

5 Yaping Wu<sup>1</sup>, Furong Yue<sup>2</sup>, Juntian Xu<sup>2,\*</sup>, John Beardall<sup>3</sup>

6 1. College of Oceanography, Hohai University, Nanjing, 210098, China

7 2. College of Marine Life and Fisheries, Huaihai Institute of Technology, Lianyungang,  
8 222005, China

9 3. School of Biological Sciences, Monash University, Clayton, Victoria 3800, Australia

10

11

12 \* Author correspondence: [jtxu@hhit.edu.cn](mailto:jtxu@hhit.edu.cn)

13 **Abstract:**

14 We studied the photophysiological responses to ultraviolet radiation (UVR) of two  
15 diatoms, isolated from different environmental niches. Both species showed the highest  
16 sensitivity to UV radiation under relatively low temperature, while they were less  
17 inhibited under moderately increased temperature. Under the highest temperature  
18 applied in this study, the benthic diatom *Nitzschia sp.* showed minimal sensitivity to  
19 UV radiation, while inhibition of the planktonic species, *Skeletonema sp.*, increased  
20 further compared with that at the growth temperature. These photochemical responses  
21 were linked to values for the repair and damage processes within the cell; higher  
22 damage rates and lower repair rates were observed for *Skeletonema sp.* under  
23 suboptimal temperature, while for *Nitzschia sp.*, repair rates increased and damage rates  
24 were stable within the applied temperature range. Our results suggested that the  
25 response of the microalgae to UV radiation correlated with their niche environments,  
26 the periodic exposure to extreme temperatures promoting the resistance of the benthic  
27 species to the combination of high temperature and UV radiation.

28

29 **Keywords:** Diatom, Photosynthetic performance, Temperature, UV radiation

30

31

32

33

34

35 **Introduction**

36 As the most abundant group of microalgae, and one that plays an important role in  
37 marine ecosystem function and biogeochemical cycles, diatoms are traditionally  
38 divided into centric and pennate species on the basis of their valve symmetry (Round  
39 et al., 1990). Centric diatoms are usually, though not invariably, planktonic and pennate  
40 species are benthic, and are often found living in different niches (Irwin et al., 2012;  
41 Keithan et al., 1988). The distribution of centric diatoms is more widespread, with  
42 records for the open ocean as well as coastal water, and they maintain their position in  
43 the upper mixing layer by maintaining buoyancy with elaborated spines or excretion of  
44 heavy ions (Lavoie et al., 2016; Villareal, 1988). In contrast, pennate diatoms are often  
45 found in the intertidal zone (Stevenson, 1983). Therefore, the 2 groups of diatom are  
46 likely to have evolved different strategies to cope with their niche environments  
47 (Barnett et al., 2015; Lavaud et al., 2016; Lavaud et al., 2007).

48 Temperature affects almost all biochemical reactions in living cells, and is one of  
49 the most important factors that determines the biogeography, as well as the temporal  
50 variation of phytoplankton (Levasseur et al., 1984). Under global change scenarios,  
51 increases in sea surface temperature would re-structure the phytoplankton assemblages  
52 in the future ocean (Thomas et al., 2012). At small spatial scales, e.g. the coastal zone,  
53 diurnal cycle of tides or meteorological events could expose benthic diatoms to extreme  
54 environments, including high photosynthetically active radiation (PAR) and ultraviolet  
55 (UV) radiation exposure as well as larger variations in temperature than found for  
56 planktonic species. Hence organisms in such exposed areas should potentially possess  
57 highly efficient mechanisms to adapt such environment (Souffreau et al., 2010; Weisse  
58 et al., 2016).

59 In the intertidal zone, UV radiation (UVR) is another driving force. UVR is a  
60 component of the solar spectrum, along with photosynthetically active radiation (PAR),  
61 and has wide reaching effects on organisms, especially photoautotrophs due to their  
62 demands for light energy (Williamson et al., 2014). The penetration of effective UVR  
63 in coastal waters is mainly dependent on the properties of the seawater (Tedetti and

64 Sempere, 2006). Previous studies have found that UVR significantly inhibited carbon  
65 fixation by phytoplankton in the surface layer, with less inhibition or even stimulation  
66 in deep water due to low UVR and limiting levels of PAR (Gao et al., 2007).  
67 Detrimental effects, however, varied seasonally, with less inhibition observed for  
68 planktonic assemblages during summer, though UV radiation was the highest. This may  
69 be attributable to the higher water temperature which facilitated enzyme-catalyzed  
70 repair processes within the cell (Wu et al., 2010). There are few documented studies on  
71 benthic species, which actually are potentially more resistant to UVR as they are  
72 periodically exposed to high solar radiation during low tide (Barnett et al., 2015).

73       Photosystem II (PSII) initiates the first step of photosynthesis, converting photons  
74 to electrons efficiently, but this complex is very sensitive to light (Campbell and  
75 Tyystjarvi, 2012). The subunits of PSII are broken down under UVR or high PAR while  
76 repaired by insertion of de-novo synthesized protein (Aro et al., 1993); the repair  
77 process eventually reaches a dynamic balance with damage (Heraud and Beardall,  
78 2000). However, these two processes are independent from each other. The  
79 photochemical damage is mainly determined by the intensity and spectrum of light  
80 (Heraud and Beardall, 2000) and is temperature insensitive, while the repair process is  
81 driven by a series of enzyme-catalyzed reactions, and is thus potentially sensitive to  
82 temperature changes (Melis, 1999). Previous studies revealed that high temperature  
83 alleviated UV inhibition of PSII in green algae (Wong et al., 2015), while it interactively  
84 decreased photosynthetic activity in microphytobenthos under excessive PAR  
85 conditions (Laviale et al., 2015).

86       Considering the importance of diatoms to coastal primary productivity  
87 (Carstensen et al., 2015), their responses to environmental factors are of considerable  
88 interest (Häder et al., 2011). However, the niches in which planktonic and benthic  
89 diatom species exist have quite different physical and chemical characteristics  
90 (Souffreau et al., 2010). In this study, we used two freshly isolated species to test the  
91 hypothesis that benthic diatoms have a stronger ability to adapt to potentially stressful  
92 solar UV radiation under high temperature regimes.

93

## 94 **Materials and methods**

### 95 1. Species and culture conditions

96 We collected samples from offshore water and intertidal sediments in the coastal  
97 area of the Yellow Sea. These were re-suspended in seawater, and enriched with Aquil  
98 medium and incubated in a growth chamber for 3 days (Morel et al., 1979). Then a sub-  
99 sample was examined under a microscope, and single cells were picked up with a micro  
100 pipette. *Skeletonema sp.* and *Nitzschia sp.* were chosen for the present study, and were  
101 maintained in Aquil medium in a growth chamber at 15 °C. Prior to the experiment,  
102 both species were inoculated into enriched seawater (Aquil medium) and cultured semi-  
103 continuously in 500 mL polycarbonate bottles, illuminated with cool fluorescent tubes  
104 at a photon flux density of  $\sim 200 \mu\text{mol m}^{-2} \text{s}^{-1}$ , with a 12:12 light/dark cycle. Temperature  
105 was set at 15, 20 or 25 °C, with variation less than 0.5 °C, and cultures were diluted  
106 every day with fresh medium. Bottles (triplicates for each temperature) were manually  
107 shaken 2–3 times during the light period and randomly distributed in the growth  
108 chamber.

109 Specific growth rate was estimated from the changes of dark adapted chlorophyll  
110 fluorescence (see below), and calculated as:  $\mu = (\text{Ln } F_2 - \text{Ln } F_1) / (D_2 - D_1)$ , where  $F_1$   
111 and  $F_2$  represent the steady-state fluorescence intensity at day 1 or day 2, respectively.

112

### 113 2. Determination of the absorption spectra of pigments

114 50 mL of culture was filtered onto a GF/F filter, and extracted in 5 mL absolute  
115 methanol for 2 h at room temperature in a 10 mL centrifuging tube, then centrifuged at  
116 4000 rpm for 15 min (TDZ4-WS, Luxiang Inc.). The supernatant was scanned with a  
117 spectrophotometer (Lambda 35, PerkinElmer) in the range of 280nm-750 nm.

### 118 3. Experimental set up

119 The experiments were performed under a customized solar simulator with a 1,000  
120 W xenon arc lamp as the light source. The incident irradiances of UV-B light (280–315  
121 nm), UV-A (315–400 nm), and PAR (400–700 nm) were measured using a broadband

122 radiometer (SOLAR-2UV, TINEL Inc. , <http://www.tinel.cn>).

123 After 5 days acclimation under the target temperature, samples of both species in  
124 the exponential phase were harvested during the middle of the light period, and directly  
125 transferred to quartz tubes (35 mL) at a density of less than 20  $\mu\text{g chl } a \text{ L}^{-1}$ , dark-adapted  
126 for 15 min, and treated by addition of milli-Q water (as a control) or lincomycin (final  
127 concentration, 0.5 mg mL<sup>-1</sup>); the latter inhibits protein synthesis and was used to get a  
128 better determination of damage rate in the absence of repair. The tubes were then placed  
129 into a water bath one after another at 1 minute intervals while covered with cut-off  
130 filters (ZJB280, ZJB400) that block radiation below 280 or 400 nm, respectively (the  
131 filters properties were checked by scanning in the wavelength range of 280-750 nm  
132 against air as a blank, see Figure A1), to create PAR + UV-A + UV-B (PAB) and PAR  
133 (P) treatments respectively. The light levels applied were PAR = 440  $\mu\text{mol photons m}^{-2}$   
134 s<sup>-1</sup> and UVR = 41.6 W m<sup>-2</sup>, while temperature was controlled with a cooling system  
135 (CTP3000, Eyela) and was set as the incubation level (termed “acclimated”) or the  
136 incubation temperature +10 °C (termed “short term”), the latter mimicking a moderate  
137 increase in temperature in the intertidal zone during a low tide period. After the light  
138 exposure, samples were moved into a water bath at the same temperature as light  
139 exposure, but under dim light ( $\sim 30 \mu\text{mol photons m}^{-2} \text{ s}^{-1}$ ), for recovery, effective  
140 quantum yields were then measured at 12 min intervals. The detailed experimental  
141 design can be found in Fig A2 in the supplementary information.

#### 142 4. Chlorophyll fluorescence measurements

143 A total of 12 tubes (2 species and 2 radiation treatments for each temperature level)  
144 were dark-adapted for 15 min, then each tube was moved into a water bath one by one  
145 at 1 minute intervals for light exposure, and 2 mL sub-samples were taken to measure  
146 the initial chlorophyll fluorescence with an Aquapen fluorometer (AP-C 100, PSI).  
147 During the subsequent light exposure, sub-samples were withdrawn every 12 minutes  
148 from the quartz tubes for fluorescence measurement; this procedure ensured that every  
149 sample was exposed to radiation for exactly the same time. After five rounds of  
150 measurements (60 min), samples that were without lincomycin were transferred into

151 the low light condition under the same temperature for recovery, and chlorophyll  
152 fluorescence was measured as above for 60 min.

## 153 5. Data analysis

154 Effective quantum yields were measured after 20 s of dark period (operational time  
155 between sampling and measuring) with the AquaPen and calculated according to the  
156 following equations:

$$157 \quad \text{Effective quantum yield} = (F_m' - F_o') / F_m'$$

158 where  $F_m'$  is the effective maximal fluorescence, and  $F_o'$  is the minimal fluorescence in  
159 the presence of nonphotochemical quenching which persists after highlight exposure.

160 The relative UV inhibition of effective quantum yield was estimated according to  
161 the following equation:

$$162 \quad \text{Relative UV inhibition (\%)} = (P_P - P_{PAB}) / P_P \times 100,$$

163 where  $P_P$  and  $P_{PAB}$  represent the effective quantum yield under P and PAB treatments,  
164 respectively. Relative UV inhibition was calculated when  $P_P$  and  $P_{PAB}$  were significantly  
165 different.

166 The rates of UVR-induced damage to PSII ( $k$ ,  $\text{min}^{-1}$ ) were calculated from  
167 lincomycin treated samples assuming repair ( $r$ ) under these conditions was zero.  
168 Repair rates ( $r$ ,  $\text{min}^{-1}$ ) were calculated using non-lincomycin-treated samples with the  
169 fixed  $k$  values obtained from the parallel experiments with lincomycin. Both  
170 calculations were made according to the Kok equation (Heraud and Beardall, 2000):

$$171 \quad \frac{P_t}{P_0} = \frac{r}{k+r} + \frac{k}{k+r} e^{-(k+r)t},$$

172 where  $P_0$  and  $P_t$  represent the effective quantum yield at time zero and  $t$  (minutes),  
173 respectively.

174 The recovery rates under dim light were calculated with a simple exponential rise  
175 equation (Heraud and Beardall, 2000):

$$176 \quad y = y_0 + c (1 - e^{-\alpha t})$$

177 where  $y$  represents the effective quantum yield at time  $t$  (minutes) during the dim  
178 light incubation,  $\alpha$  was the recovery rate, while  $y_0$  and  $c$  are constants.

179 Statistical differences for the kinetics of changes in effective quantum yield among

180 treatments were analyzed with repeated measures analysis of variance (RM-ANOVA).  
181 The differences of relative UV inhibition and rate constants among treatments were  
182 analyzed by one-way ANOVA; a confidence interval of 95% was set for all tests. For  
183 the calculation of the ratio of  $r : k$  and the relative UV inhibition (%), propagation errors  
184 were taken into account to estimate variance.

185

## 186 **Results**

187 The initial photochemical quantum yield of *Skeletonema sp.* grown at 15 °C was  
188 around 0.50 during light exposure (incubated under 15 °C), but decreased gradually  
189 toward the end of the radiation treatments, with lower values under PAB than under the  
190 P condition ( $p < 0.001$ ,  $F = 30.1$ ) (Fig 1A, Table A1). During the dim light exposure period,  
191 the quantum yield recovered to its initial value within 24 min under P treatment, while  
192 PAB treated cells only recovered partially to ~70% by the end of the dim light  
193 incubation (Fig 1A). For 15 °C grown cells that were incubated under 25 °C, the general  
194 patterns were similar to those incubated under 15 °C; the differences between the P and  
195 PAB treatments was smaller but still significant ( $p < 0.001$ ,  $F = 9.8$ ) (Fig 1B, Table A1).  
196 Under dim light, the quantum yield of cells under both radiation treatments recovered  
197 to near initial values (Fig 1B). For 15 °C grown *Nitzschia sp.* that was measured at  
198 15 °C, the pattern of decrease in effective quantum yield was similar to that of  
199 *Skeletonema sp.*, with lower values under PAB ( $p < 0.001$ ,  $F = 38.8$ ) (Fig 1C, Table A1).  
200 In addition, PAB exposed *Nitzschia sp.* could only recover to ~50% of the initial value  
201 under dim light (Fig 1C). However, when 15 °C grown *Nitzschia sp.* were incubated at  
202 25 °C for light exposure, both P and PAB treated cells had higher quantum yields, and  
203 PAB exposed cells recovered to 75% of the initial value when subsequently incubated  
204 under dim light (Fig 1D). The increase of temperature (15 to 25 °C) and UV radiation  
205 also showed interactive effects for both *Skeletonema sp.* ( $p = 0.022$ ,  $F = 2.98$ ) and  
206 *Nitzschia sp.* ( $p = 0.046$ ,  $F = 2.5$ ) (Table A2).

207 The 20 °C grown *Skeletonema sp.* showed significant UV inhibition at incubation



208 temperatures of 20°C ( $p<0.001$ ,  $F=8.9$ ) and 30 °C ( $p=0.033$ ,  $F=3.1$ ), and recovered  
209 more quickly under dim light, especially for the PAB treated cells, compared with  
210 samples under 15 °C (Fig 2 A, B, Table A1). For *Nitzschia sp.* that were grown at 20 °C,  
211 cells showed moderate UV inhibition during radiation exposure ( $p<0.001$ ,  $F=10.1$ ), and  
212 the quantum yield under PAB treatment only recovered to ~80% at the end of the dim  
213 light incubation at 20 °C, while quantum yield recovered to the initial value in cells  
214 measured under 30 °C (Fig 2 C, D, Table A1). Interactive effects of temperature  
215 increase (20 to 30 °C) and UV radiation were observed for both *Skeletonema sp.*  
216 ( $p<0.01$ ,  $F=4.35$ ) and *Nitzschia sp.* ( $p=0.015$ ,  $F=3.26$ ) (Table A2).

217 *Skeletonema sp.* that was grown and measured at 25 °C showed a similar pattern  
218 to that grown under 20 °C during both radiation exposure and subsequent dim light (Fig  
219 3A). However, quantum yields decreased significantly once cells were moved into  
220 35 °C, with much lower values observed under the PAB and P treatments ( $p<0.001$ )  
221 than under 25 °C. However, there was no significant difference between PAB and P  
222 treatments under 35 °C ( $p=0.60$ ,  $F=0.74$ ) (Table A1). During the dim light period,  
223 *Skeletonema sp.* only recovered to ~30% for the P treatment, while there was no  
224 recovery after the PAB treatment (Fig 3B). For *Nitzschia sp.* measured under 25 or  
225 35 °C, both treatments showed a similar response, with lower values under PAB than  
226 under P during the radiation exposure ( $p<0.001$  and  $F=13.3$  at 25 °C,  $p<0.01$  and  $F=5.4$   
227 at 35 °C) (Table A1), while cells could recover to near initial values at the end of the  
228 dim light incubation (Fig 3 C, D). An interactive effect of temperature increase (25-  
229 35 °C) and UV radiation was only observed for *Skeletonema sp.* ( $p=0.049$ ,  $F=2.46$ )  
230 (Table A2).

231 In the presence of lincomycin, changes in effective quantum yield showed a  
232 decreasing pattern with exposure time for most of the treatments (Figure A3-5), but  
233 with much greater amplitude compared with non-lincomycin treated samples. The  
234 relative UV inhibition at the end of radiation exposure is shown in Fig 4. Both species  
235 showed the greatest sensitivities under 15 °C, with ~80% and ~70% relative UV  
236 inhibition of photochemical quantum yield for *Skeletonema sp.* and *Nitzschia sp.*,

237 respectively. In the range of acclimated temperatures, relative UV inhibition decreased  
238 with increase of temperature for both species. In the short term incubations with a 10 °C  
239 increase, UV inhibition of *Skeletonema sp.* was comparable at 25 °C and 30 °C, but  
240 increased significantly to ~50% at 35 °C ( $p<0.01$ ). For *Nitzschia sp.*, relative UV  
241 inhibition was around 25% in the temperature range of 25 – 35 °C during the short term  
242 incubations.

243 During radiation exposure, the repair rates for PSII in *Skeletonema sp.* varied  
244 across the different temperatures, with highest values observed at 25 °C, and lowest  
245 values at 35 °C for both radiation treatments (Fig 5A). The damage rates gradually  
246 decreased from 15 to 25 °C, then increased significantly toward 35 °C (Fig 5B)  
247 ( $p<0.001$ ). The ratio of repair rate to damage rate ( $r : k$ ) showed a unimodal pattern with  
248 peak values at 25 °C, and with lowest values under 15 or 35 °C, especially for the PAB  
249 treatment (Fig 5C).

250 The repair rate during light exposure for *Nitzschia sp.*, increased significantly in  
251 the temperature range of 15 to 25 °C ( $p<0.001$ ), while kept relatively stable from 25 to  
252 35 °C (Fig 6A). The damage rates were quite stable for all temperatures tested, whether  
253 cells were acclimated or exposed to short term elevation of temperature, with mean  
254 values around 0.075 for PAB and 0.032 for P treatment (Fig 6B). The  $r : k$  ratio  
255 increased with temperature in the range of 15-25 °C, reaching relatively stable values  
256 of around 1.50 for P, and around 1.0 for the PAB treatment (Fig 6C).

257 Under dim light, the rate constants for recovery of P-exposed *Skeletonema sp.*  
258 were around 0.10-0.15  $\text{min}^{-1}$  in the range of 15-30 °C, but increased significantly to  
259 around 0.30 at 35 °C ( $p<0.01$ ) (Fig 7A). The rate constant for recovery of P exposed  
260 *Nitzschia sp.* was relatively stable, around 0.25  $\text{min}^{-1}$ , across the range of applied  
261 temperature (Fig 7B). The rate constant for recovery of PAB exposed *Skeletonema sp.*  
262 showed an increasing pattern from 0.05 to 0.17  $\text{min}^{-1}$  in the range of 15-25 °C, but  
263 decreased significantly at 30 °C ( $p<0.05$ ); at 35° values were unable to be estimated  
264 due to poor fitting of data points (Fig 7C). No consistent trend was found for the rate  
265 constant for recovery of PAB exposed *Nitzschia sp.*, which varied around 0.10-0.15

266 min<sup>-1</sup>, across the range of applied temperature (Fig 7D).

267

## 268 **Discussion**

269 In the present study, we found that both benthic and planktonic diatoms were less  
270 inhibited by UVR under moderately increased temperature, while the benthic species  
271 was more resistant to UVR under the highest temperature applied, which suggests that  
272 the tolerance to environmental stress was associated with the niche environment where  
273 the microalgae are living, that would be in turn determine the biogeographic properties  
274 of the species. These findings imply that temperature is a key factor that mediates the  
275 response of diatoms to UVR, while different species have developed distinct  
276 mechanisms in response to their particular niche environments (Laviale et al., 2015).

277 As a basic environmental factor, temperature affects all metabolic pathways, and  
278 extreme or sub-optimal conditions are often encountered by various organisms in nature  
279 (Mosby and Smith, 2015). The growth response of phytoplankton to temperature varies  
280 from species to species, but often shows a unimodal pattern (Brown et al., 2004; Chen,  
281 2015). For the applied temperature range in the present study, the growth rate of the  
282 benthic species showed a slight response, while growth increased with temperature to  
283 a greater extent in the planktonic species, particularly above 25 °C. However, life forms  
284 in the natural environment are affected by multiple stressors concomitantly (Boyd et al.,  
285 2015). For instance, recent studies have demonstrated that increased temperature would  
286 affect phytoplankton interactively with light intensity (Edwards et al., 2016), and could  
287 alleviate UV direct inhibition in some sensitive species (Halac et al., 2014). Moreover,  
288 in diatoms short-term changes in temperature showed a greater interaction with UV  
289 radiation than did long-term exposure, which was particularly important for intertidal  
290 benthic species (Sobrino and Neale, 2007). In the present study, when species were  
291 acclimated under sub-optimal temperature (15 °C), both showed obvious sensitivity to  
292 UVR (Fig 1). During the recovery period, however, the effective quantum yield of the  
293 benthic diatom could rapidly regain the highest values within 12 min irrespective of the  
294 incubation temperature. The planktonic diatom, however, only performed better under

295 short-term elevated temperature. This suggests that the benthic species could have  
296 broader adaptability to cope with the highly varied temperature environment they  
297 frequently experience (Laviale et al., 2015).

298 The operation of PSII is sensitive to light intensity as well as quality. High levels  
299 of PAR and UVR can usually induce significant damage to this complex, while the de  
300 novo synthesis of protein can replace the damaged subunit (Aro et al., 1993; Lavaud et  
301 al., 2016). The damage rate ( $k$ ), which represents the efficiency of detrimental effects,  
302 showed a different response for the 2 species in this study; in the planktonic species,  $k$   
303 was sensitive to temperature change, with the lowest value at the medium temperature,  
304 but was quite stable in the benthic species at all temperatures tested. This could be  
305 attributed to a decrease in electron transport, or intrinsic differences between benthic  
306 and planktonic species (Melis, 1999; Nitta et al., 2005), since  $k$  of the planktonic  
307 *Thalassiosira sp.* also showed sensitivity to temperature change (Sobrinho and Neale,  
308 2007). The repair rates ( $r$ ) and the ratio of  $r$  to  $k$  further demonstrated that the planktonic  
309 species had a relatively lower optimal temperature in response to UVR, with the highest  
310  $r : k$  and lowest UV inhibition at 25 °C. In contrast, in the benthic species  $r$  and  $r : k$   
311 increased steadily and reached relatively stable values at the highest temperature, and  
312 this coincided with lower UV inhibition, implying that although acclimated in  
313 laboratory conditions for weeks, this species still had an active mechanism to respond  
314 to high temperature and UVR, as might occur in its natural niche environment (Laviale  
315 et al., 2015).

316 In addition to repair processes that are initiated after damage, UV absorbing  
317 compounds could directly screen out part of the detrimental radiation, protecting  
318 cellular organelles from UV damage (Garcia-Pichel and Castenholz, 1993). In diatoms,  
319 however, the spectra of methanol extracts showed only a small absorbance peak in the  
320 UVR. Unlike xanthophyll cycle related pigments, UV-absorbing compounds (UVAC)  
321 are inducible and only synthesized under long-term UV exposure, indicating that UVAC  
322 are not a major protecting mechanism for laboratory cultured diatoms (Helbling et al.,  
323 1996). However, the xanthophyll cycle could respond quickly under photo-inhibitory

324 conditions, and has been shown to be a major mechanism in diatoms in response to high  
325 light or UV (Cartaxana et al., 2013; Zudaire and Roy, 2001). Therefore, the relatively  
326 higher absorption in the blue range for benthic species might indicate that temperature  
327 enhances the synthesis of xanthophyll related pigments (Havaux and Tardy, 1996). The  
328 differences in absorption spectra of extracted pigments suggests that to better  
329 understand the spectral-dependent responses to UV radiation, biological weighting  
330 functions should be introduced in this kind of work (Neale et al., 2014).

331 The temperature dependent response to UVR has major implications for  
332 phytoplankton. With the continuing emission of greenhouse gases, the surface seawater  
333 temperature is predicted to increase by up to 4 °C by the end of this century (New et al.,  
334 2011), and this could potentially re-shape the phytoplankton assemblages (Thomas et  
335 al., 2012). While the situation might be more complex in the natural environment with  
336 the consideration of interaction of UVR with other factors (Beardall et al., 2009), for  
337 unicellular green algae, an increase of temperature could mitigate UVR harm for  
338 temperate species, while exacerbating UV inhibition for polar species (Wong et al.,  
339 2015). Moreover, the tolerance of phytoplankton to extreme temperature would be  
340 latitude dependent; for tropical areas where the temperature is already high, an increase  
341 of temperature reduced the richness of phytoplankton (Thomas et al., 2012).

342 The present study showed a differential response to UV radiation for two diatoms  
343 from contrasting niches. As predicted, the benthic species had a higher tolerance to the  
344 combination of extreme temperature and UV radiation, which can be attributed to the  
345 environment in which were living. Below the optimal temperature, both species  
346 performed better in response to UV radiation under elevated temperature, suggesting  
347 that the natural variation of temperature due to changes in the heat flux from the sun or  
348 meteorological events would alter the extent of UV effects on primary producers, and  
349 therefore the aquatic ecosystem (Häder et al., 2011). Furthermore, considering the  
350 projected global warming scenarios, UV radiation could impose different impacts on  
351 phytoplankton with respect to the regional differences (Beardall et al., 2009; Xie et al.,  
352 2010).

353        *Acknowledgement:* This study was supported by the National Natural Science  
354        Foundation of China (41476097) and the Fundamental Research Funds for the Central  
355        Universities (2016B12814).

356

357 **References:**

- 358 Aro, E. M., Virgin, I., and Andersson, B.: Photoinhibition of Photosystem II. Inactivation, protein  
359 damage and turnover, *Biochimica et Biophysica Acta-Bioenergetics*, 1143, 113-134,  
360 10.1016/0005-2728(93)90134-2, 1993.
- 361 Barnett, A., Meleder, V., Blommaert, L., Lepetit, B., Gaudin, P., Vyverman, W., Sabbe, K., Dupuy,  
362 C., and Lavaud, J.: Growth form defines physiological photoprotective capacity in intertidal  
363 benthic diatoms, *ISME Journal*, 9, 32-45, 10.1038/ismej.2014.105, 2015.
- 364 Beardall, J., Sobrino, C., and Stojkovic, S.: Interactions between the impacts of ultraviolet radiation,  
365 elevated CO<sub>2</sub>, and nutrient limitation on marine primary producers, *Photochemical &*  
366 *Photobiological Sciences*, 8, 1257-1265, 10.1039/b9pp00034h, 2009.
- 367 Boyd, P. W., Lennartz, S. T., Glover, D. M., and Doney, S. C.: Biological ramifications of climate-  
368 change-mediated oceanic multi-stressors, *Nature Climate Change*, 5, 71-79,  
369 10.1038/nclimate2441, 2015.
- 370 Brown, J. H., Gillooly, J. F., Allen, A. P., Savage, V. M., and West, G. B.: Toward a metabolic theory  
371 of ecology, *Ecology*, 85, 1771-1789, 10.1890/03-9000, 2004.
- 372 Campbell, D. A., and Tyystjarvi, E.: Parameterization of photosystem II photoinactivation and repair,  
373 *Biochimica et Biophysica Acta -Bioenergetics*, 1817, 258-265, 10.1016/j.bbatio.2011.04.010,  
374 2012.
- 375 Carstensen, J., Klais, R., and Cloern, J. E.: Phytoplankton blooms in estuarine and coastal waters:  
376 Seasonal patterns and key species, *Estuarine Coastal and Shelf Science*, 162, 98-109,  
377 10.1016/j.ecss.2015.05.005, 2015.
- 378 Cartaxana, P., Domingues, N., Cruz, S., Jesus, B., Laviale, M., Serodio, J., and da Silva, J. M.:  
379 Photoinhibition in benthic diatom assemblages under light stress, *Aquatic Microbial Ecology*,  
380 70, 87-92, 10.3354/ame01648, 2013.
- 381 Chen, B.: Patterns of thermal limits of phytoplankton, *Journal of Plankton Research*, 37, 285-292,  
382 10.1093/plankt/fbv009, 2015.
- 383 Edwards, K. F., Thomas, M. K., Klausmeier, C. A., and Litchman, E.: Phytoplankton growth and  
384 the interaction of light and temperature: A synthesis at the species and community level,  
385 *Limnology and Oceanography*, 61, 1232-1244, 10.1002/lno.10282, 2016.
- 386 Gao, K., Wu, Y., Li, G., Wu, H., Villafane, V. E., and Helbling, E. W.: Solar UV radiation drives  
387 CO<sub>2</sub> fixation in marine phytoplankton: A double-edged sword, *Plant Physiology*, 144, 54-59,  
388 10.1104/pp.107.098491, 2007.
- 389 Garcia-Pichel, F., and Castenholz, R. W.: Occurrence of UV-Absorbing, Mycosporine-like  
390 compounds among cyanobacterial isolates and an estimate of their screening capacity, *Applied*  
391 *and Environmental Microbiology*, 59, 163-169, 1993.
- 392 Häder, D.-P., Helbling, E., Williamson, C., and Worrest, R.: Effects of UV radiation on aquatic  
393 ecosystems and interactions with climate change, *Photochemical & Photobiological Sciences*,  
394 10, 242-260, 2011.
- 395 Halac, S. R., Villafane, V. E., Goncalves, R. J., and Helbling, E. W.: Photochemical responses of  
396 three marine phytoplankton species exposed to ultraviolet radiation and increased temperature:  
397 Role of photoprotective mechanisms, *Journal of Photochemistry and Photobiology B-Biology*,  
398 141, 217-227, 10.1016/j.jphotobiol.2014.09.022, 2014.
- 399 Havaux, M., and Tardy, F.: Temperature-dependent adjustment of the thermal stability of  
400 photosystem II in vivo: Possible involvement of xanthophyll-cycle pigments, *Planta*, 198, 324-

333, 10.1007/bf00620047, 1996.

Helbling, E. W., Chalker, B. E., Dunlap, W. C., HolmHansen, O., and Villafane, V. E.: Photoacclimation of Antarctic marine diatoms to solar ultraviolet radiation, *Journal of Experimental Marine Biology and Ecology*, 204, 85-101, 10.1016/0022-0981(96)02591-9, 1996.

Heraud, P., and Beardall, J.: Changes in chlorophyll fluorescence during exposure of *Dunaliella tertiolecta* to UV radiation indicate a dynamic interaction between damage and repair processes, *Photosynthesis Research*, 63, 123-134, 10.1023/a:1006319802047, 2000.

Irwin, A. J., Nelles, A. M., and Finkel, Z. V.: Phytoplankton niches estimated from field data, *Limnology and Oceanography*, 57, 787-797, 10.4319/lo.2012.57.3.0787, 2012.

Irwin, A. J., Finkel, Z. V., Mueller-Karger, F. E., and Ghinaglia, L. T.: Phytoplankton adapt to changing ocean environments, *Proceedings of the National Academy of Sciences of the United States of America*, 112, 5762-5766, 10.1073/pnas.1414752112, 2015.

Keithan, E. D., Lowe, R. L., and DeYoe, H. R.: Benthic diatom distribution in a pennsylvania stream: role of pH and nutrients, *Journal of Phycology*, 24, 581-585, 1988.

Lavaud, J., Strzepek, R. F., and Kroth, P. G.: Photoprotection capacity differs among diatoms: Possible consequences on the spatial distribution of diatoms related to fluctuations in the underwater light climate, *Limnology and Oceanography*, 52, 1188-1194, 2007.

Lavaud, J., Six, C., and Campbell, D. A.: Photosystem II repair in marine diatoms with contrasting photophysiology, *Photosynthesis Research*, 127, 189-199, 10.1007/s11120-015-0172-3, 2016.

Laviale, M., Barnett, A., Ezequiel, J., Lepetit, B., Frankenbach, S., Meleder, V., Serodio, J., and Lavaud, J.: Response of intertidal benthic microalgal biofilms to a coupled light-temperature stress: evidence for latitudinal adaptation along the Atlantic coast of Southern Europe, *Environmental Microbiology*, 17, 3662-3677, 10.1111/1462-2920.12728, 2015.

Lavoie, M., Raven, J. A., and Levasseur, M.: Energy cost and putative benefits of cellular mechanisms modulating buoyancy in a flagellate marine phytoplankton, *Journal of Phycology*, 52, 239-251, 10.1111/jpy.12390, 2016.

Levasseur, M., Therriault, J.-C., and Legendre, L.: Hierarchical control of phytoplankton succession by physical factors, *Marine Ecology Progress Series*, 19, 211-222, 1984.

Melis, A.: Photosystem-II damage and repair cycle in chloroplasts: what modulates the rate of photodamage in vivo?, *Trends in Plant Science*, 4, 130-135, 10.1016/s1360-1385(99)01387-4, 1999.

Morel, F. M. M., Rueter, J. G., Anderson, D. M., and Guillard, R. R. L.: Aquil: a chemically defined phytoplankton culture medium for trace metal studies, *Journal of Phycology*, 15, 135-141, 10.1111/j.1529-8817.1979.tb02976.x, 1979.

Mosby, A. F., and Smith, W. O., Jr.: Phytoplankton growth rates in the Ross Sea, Antarctica, *Aquatic Microbial Ecology*, 74, 157-171, 10.3354/ame01733, 2015.

Neale, P. J., Pritchard, A. L., and Ihnacik, R.: UV effects on the primary productivity of picophytoplankton: biological weighting functions and exposure response curves of *Synechococcus*, *Biogeosciences*, 11, 2883-2895, 10.5194/bg-11-2883-2014, 2014.

New, M., Liverman, D., Schroeder, H., and Anderson, K.: Four degrees and beyond: the potential for a global temperature increase of four degrees and its implications (vol 369, pg 6, 2011), *Philosophical Transactions of the Royal Society a-Mathematical Physical and Engineering Sciences*, 369, 1112-1112, 10.1098/rsta.2010.0351, 2011.



445 Nitta, K., Suzuki, N., Honma, D., Kaneko, Y., and Nakamoto, H.: Ultrastructural stability under  
446 high temperature or intensive light stress conferred by a small heat shock protein in  
447 cyanobacteria, *FEBS Letters*, 579, 1235-1242, 10.1016/j.febslet.2004.12.095, 2005.

448 Padfield, D., Yvon-Durocher, G., Buckling, A., Jennings, S., and Yvon-Durocher, G.: Rapid  
449 evolution of metabolic traits explains thermal adaptation in phytoplankton, *Ecology Letters*,  
450 19, 133-142, 10.1111/ele.12545, 2016.

451 Round, F. E., Crawford, R. M., and Mann, D. G.: *Diatoms: Biology and Morphology of the Genera*,  
452 Cambridge University Press, 1990.

453 Sobrino, C., and Neale, P. J.: Short-term and long-term effects of temperature on photosynthesis in  
454 the diatom *Thalassiosira pseudonana* under UVR exposures, *Journal of Phycology*, 43, 426-  
455 436, 10.1111/j.1529-8817.2007.00344.x, 2007.

456 Souffreau, C., Vanormelingen, P., Verleyen, E., Sabbe, K., and Vyverman, W.: Tolerance of benthic  
457 diatoms from temperate aquatic and terrestrial habitats to experimental desiccation and  
458 temperature stress, *Phycologia*, 49, 309-324, 10.2216/09-30.1, 2010.

459 Stevenson, R. J.: Effects of current and conditions simulating autogenically changing microhabitats  
460 on benthic diatom immigration, *Ecology*, 64, 1514-1524, 10.2307/1937506, 1983.

461 Tedetti, M., and Sempere, R.: Penetration of ultraviolet radiation in the marine environment. A  
462 review, *Photochemistry and Photobiology*, 82, 389-397, 10.1562/2005-11-09-ir-733, 2006.

463 Thomas, M. K., Kremer, C. T., Klausmeier, C. A., and Litchman, E.: A global pattern of thermal  
464 adaptation in marine phytoplankton, *Science*, 338, 1085-1088, 10.1126/science.1224836, 2012.

465 Villareal, T. A.: Positive buoyancy in the oceanic diatom *Rhizosolenia debyana* H. Peragallo, *Deep*  
466 *Sea Research Part A. Oceanographic Research Papers*, 35, 1037-1045,  
467 [http://dx.doi.org/10.1016/0198-0149\(88\)90075-1](http://dx.doi.org/10.1016/0198-0149(88)90075-1), 1988.

468 Weisse, T., Groeschl, B., and Bergkemper, V.: Phytoplankton response to short-term temperature  
469 and nutrient changes, *Limnologica*, 59, 78-89, 10.1016/j.limno.2016.05.002, 2016.

470 Williamson, C. E., Zepp, R. G., Lucas, R. M., Madronich, S., Austin, A. T., Ballare, C. L., Norval,  
471 M., Sulzberger, B., Bais, A. F., McKenzie, R. L., Robinson, S. A., Haeder, D.-P., Paul, N. D.,  
472 and Bornman, J. F.: Solar ultraviolet radiation in a changing climate, *Nature Climate Change*,  
473 4, 434-441, 10.1038/nclimate2225, 2014.

474 Wong, C.-Y., Teoh, M.-L., Phang, S.-M., Lim, P.-E., and Beardall, J.: Interactive effects of  
475 temperature and UV radiation on photosynthesis of *Chlorella* strains from polar, temperate and  
476 tropical environments: Differential impacts on damage and repair, *PlosOne*, 10,  
477 10.1371/journal.pone.0139469, 2015.

478 Wu, Y., Gao, K., Li, G., and Walter Helbling, E.: Seasonal impacts of solar UV radiation on  
479 photosynthesis of phytoplankton assemblages in the coastal waters of the South China Sea,  
480 *Photochemistry and Photobiology*, 86, 586-592, 10.1111/j.1751-1097.2009.00694.x, 2010.

481 Wu, Y., Li, Z., Du, W., and Gao, K.: Physiological response of marine centric diatoms to ultraviolet  
482 radiation, with special reference to cell size, *Journal of Photochemistry and Photobiology B-*  
483 *Biology*, 153, 1-6, 10.1016/j.jphotobiol.2015.08.035, 2015.

484 Xie, S.-P., Deser, C., Vecchi, G. A., Ma, J., Teng, H., and Wittenberg, A. T.: Global warming pattern  
485 formation: Sea surface temperature and rainfall, *Journal of Climate*, 23, 966-986,  
486 10.1175/2009jcli3329.1, 2010.

487 Zudaire, L., and Roy, S.: Photoprotection and long-term acclimation to UV radiation in the marine  
488 diatom *Thalassiosira weissflogii*, *Journal of Photochemistry and Photobiology B-Biology*, 62,

489 26-34, 10.1016/s1011-1344(01)00150-6, 2001.  
490

491

492 **Fig legends:**

493 Fig 1 The quantum yields of 15 °C grown *Skeletonema sp.* and *Nitzschia sp.* under P or P+UVR for  
494 1 hour exposure and subsequent recovery under dim light (gray area) for 1 hour, that were incubated  
495 and measured at 15 °C (A: *Skeletonema sp.*, C: *Nitzschia sp.*) or 25 °C (B: *Skeletonema sp.*, D:  
496 *Nitzschia sp.*), vertical lines represent SD, n=3.

497 Fig 2 The quantum yields of 20 °C grown *Skeletonema sp.* and *Nitzschia sp.* under P or P+UVR for  
498 1 hour exposure and subsequent recovery under dim light (gray area) for 1 hour, that were incubated  
499 and measured at 20 °C (A: *Skeletonema sp.*, C: *Nitzschia sp.*) or 30 °C (B: *Skeletonema sp.*, D:  
500 *Nitzschia sp.*), vertical lines represent SD, n=3.

501 Fig 3 The quantum yields of 25 °C grown *Skeletonema sp.* and *Nitzschia sp.* under P or P+UVR for  
502 1 hour exposure and subsequent recovery under dim light (gray area) for 1 hour, that were incubated  
503 and measured at 25 °C (A: *Skeletonema sp.*, C: *Nitzschia sp.*) or 35 °C (B: *Skeletonema sp.*, D:  
504 *Nitzschia sp.*), vertical lines represent SD, n=3.

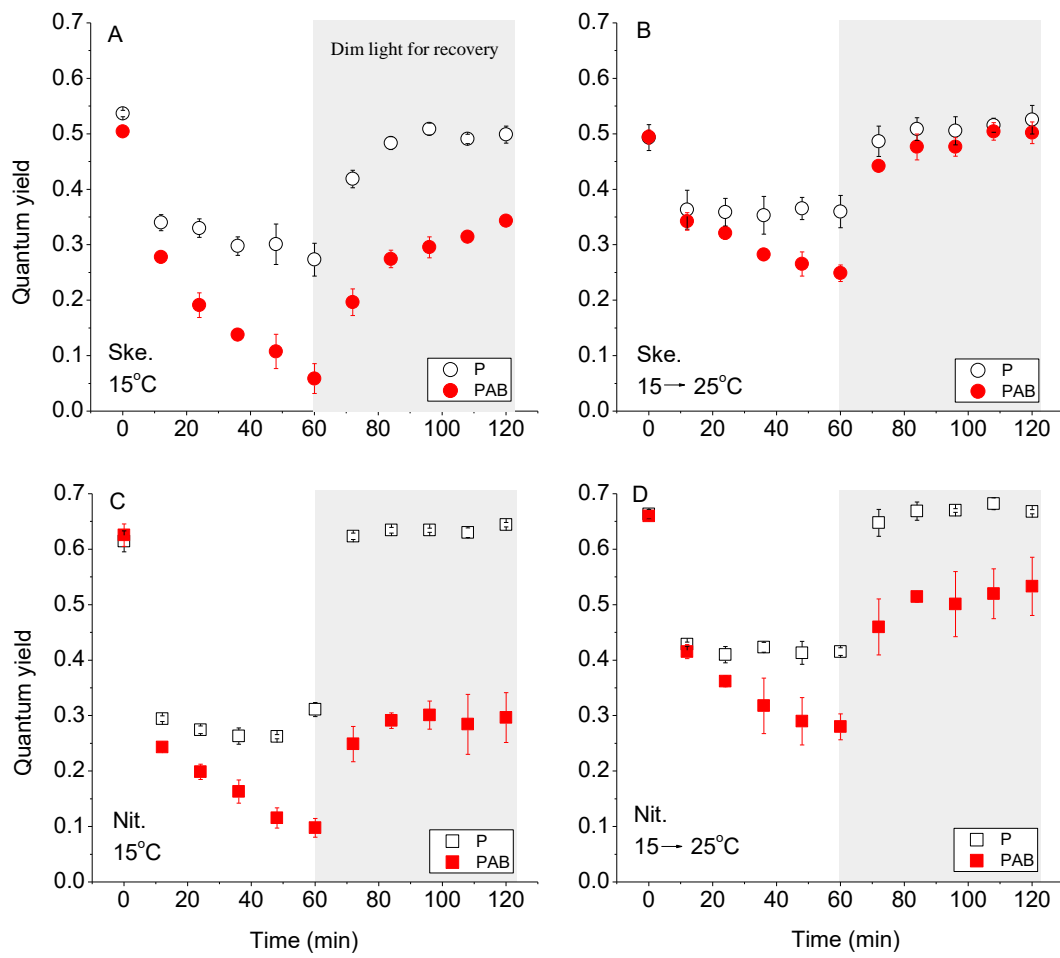
505 Fig 4 The relative UV inhibition on the photosystem II of *Skeletonema sp.* (A) and *Nitzschia sp.* (B)  
506 under grown or short term elevated temperature, vertical lines represent variance..

507 Fig 5 The repair rate (A) and damage rate (B) of photosystem II in *Skeletonema sp.* during P or  
508 P+UVR exposure under grown temperature (acclimated) or short term elevated temperature  
509 (short\_term), and the ratio of repair to damage rate (C), vertical lines in panel A and B represent SD,  
510 n=3, while vertical lines in panel C represent variance. Data points with different lower case letters  
511 (blue for P treatment, and red for PAB treatment) indicate significant differences among temperature  
512 treatments.

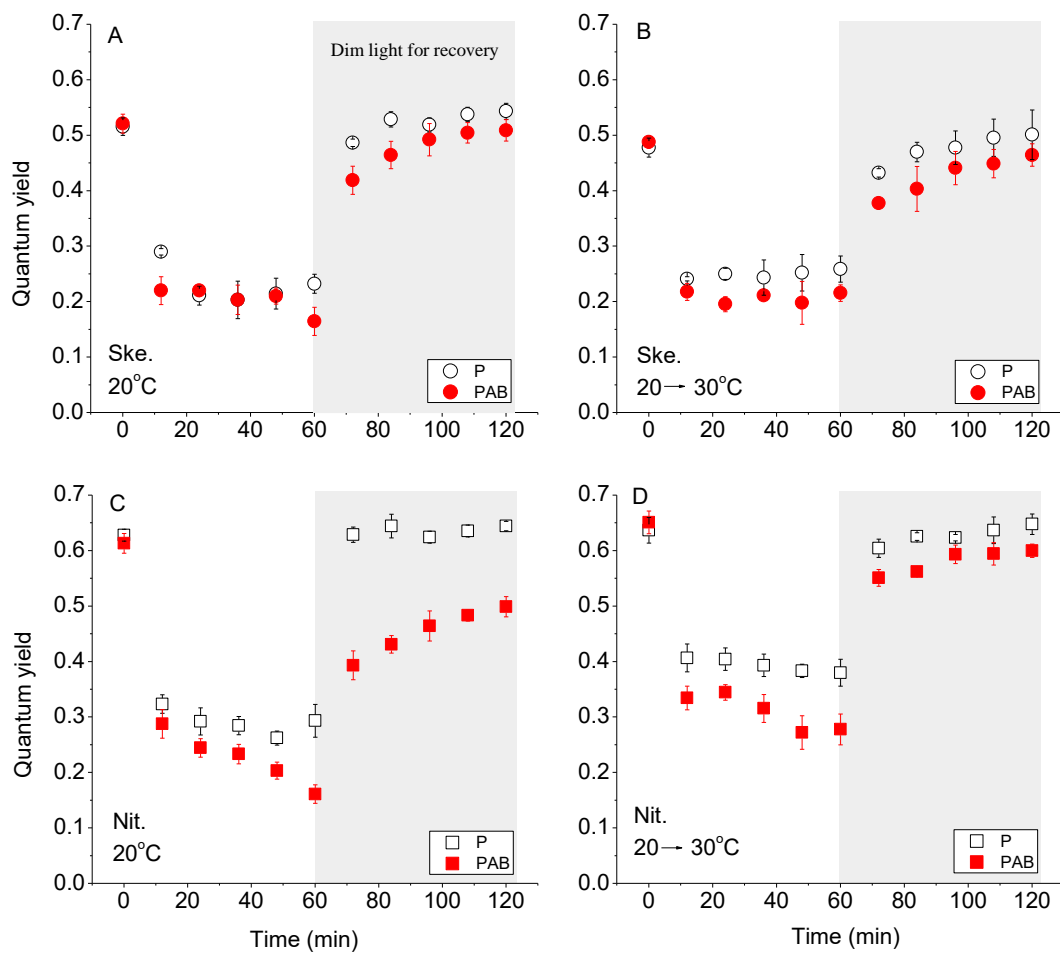
513 Fig 6 The repair rate (A) and damage rate (B) of photosystem II in *Nitzschia sp.* during P or P+UVR  
514 exposure under grown temperature (acclimated) or short term elevated temperature (short\_term),  
515 and the ratio of repair to damage rate (C), vertical lines in panel A and B represent SD, n=3, while  
516 vertical lines in panel C represent variance. Data points with different lowercase letters (blue for P  
517 treatment, and red for PAB treatment) indicated significant differences among temperature  
518 treatments.

519 Fig 7 The rate constants for recovery of P exposed *Skeletonema sp.* (A) and *Nitzschia sp.* (B), and

520 rate constants for recovery of PAB exposed *Skeletonema sp.* (C) and *Nitzschia sp.* (D) under dim  
521 light, samples were incubated under grown temperature (acclimated) or short term elevated  
522 temperature (short\_term), vertical lines represent SD, n=3. Data points with different lowercase  
523 letters (blue for P treatment, and red for PAB treatment) indicated significant differences among  
524 temperature treatments.

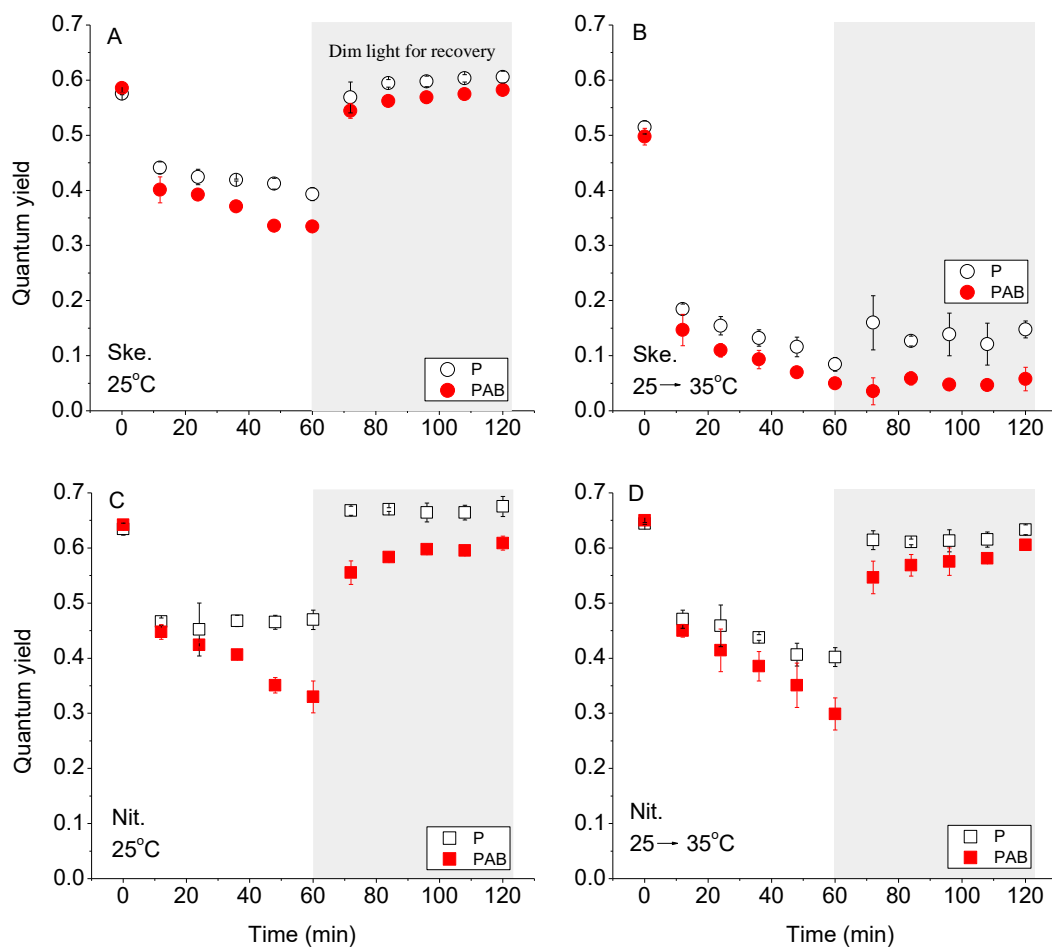


526  
 527  
 528  
 529  
 530  
 531  
 532  
 533  
 534  
 535  
 536  
 537 Fig 1  
 538



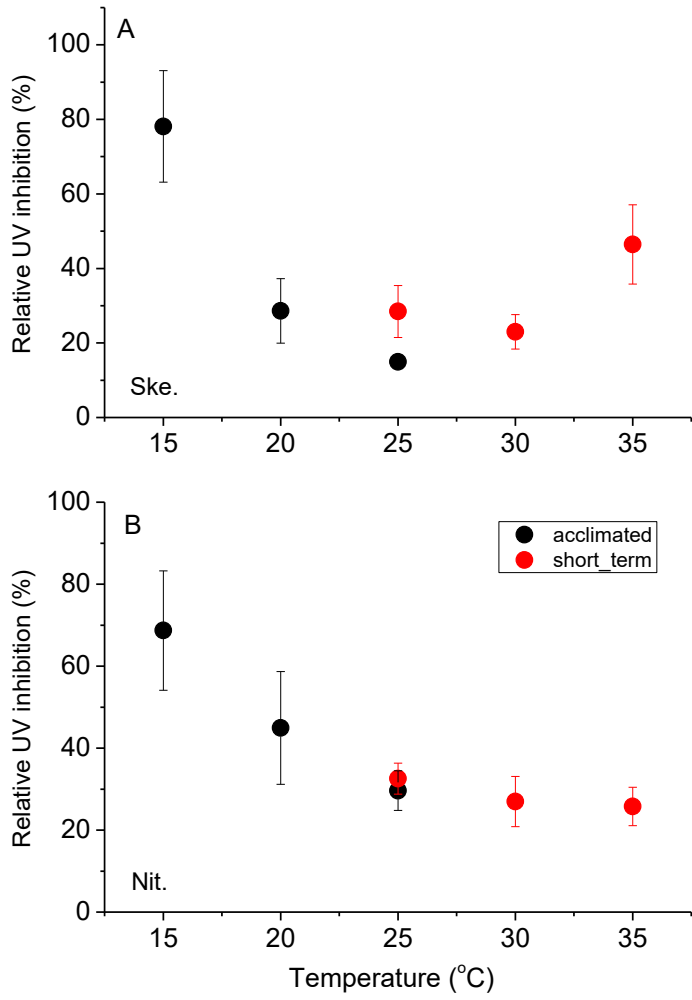
539  
 540  
 541  
 542  
 543  
 544  
 545  
 546  
 547  
 548  
 549  
 550  
 551  
 552  
 553  
 554  
 555

Fig 2



556  
 557  
 558  
 559  
 560  
 561  
 562  
 563  
 564  
 565  
 566  
 567  
 568  
 569  
 570  
 571  
 572

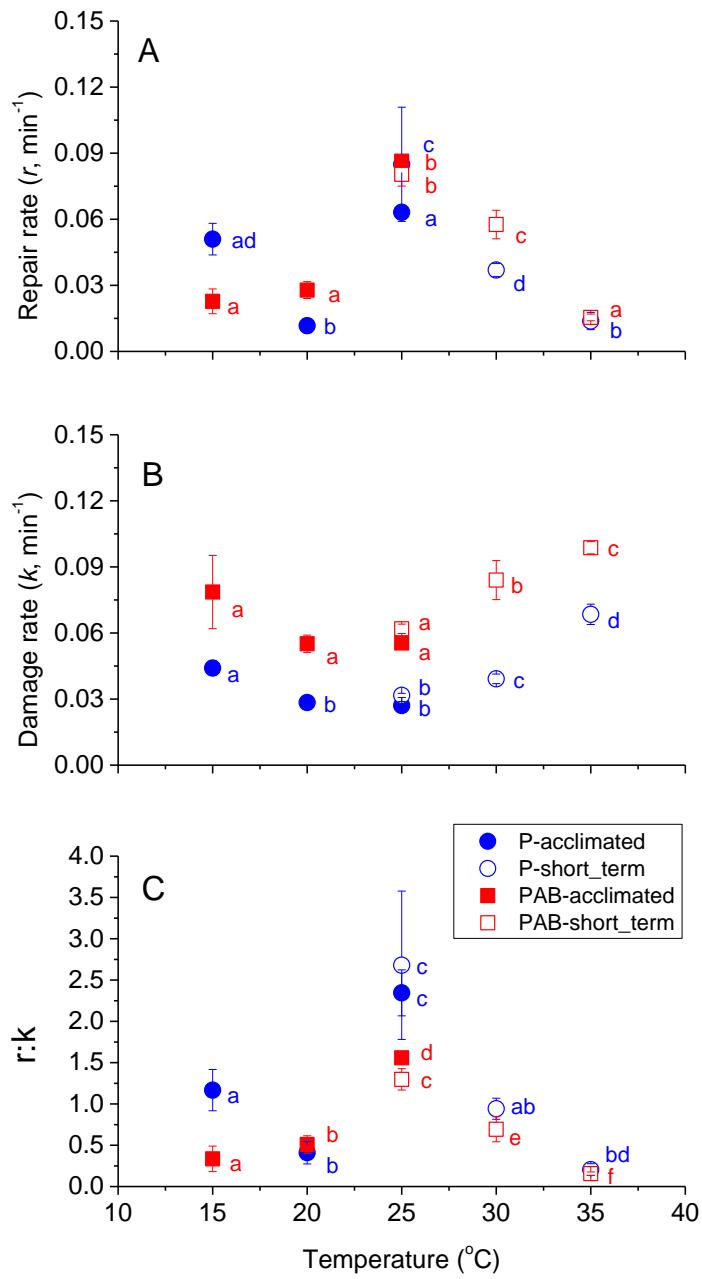
Fig 3



573  
574

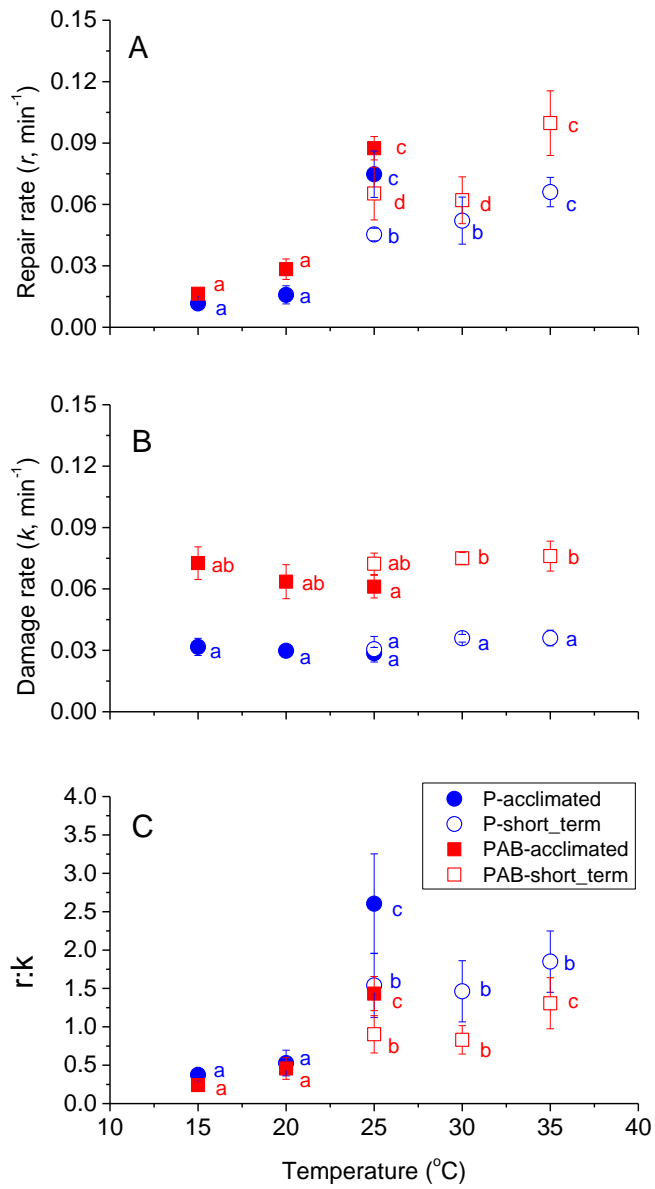
575 Fig 4





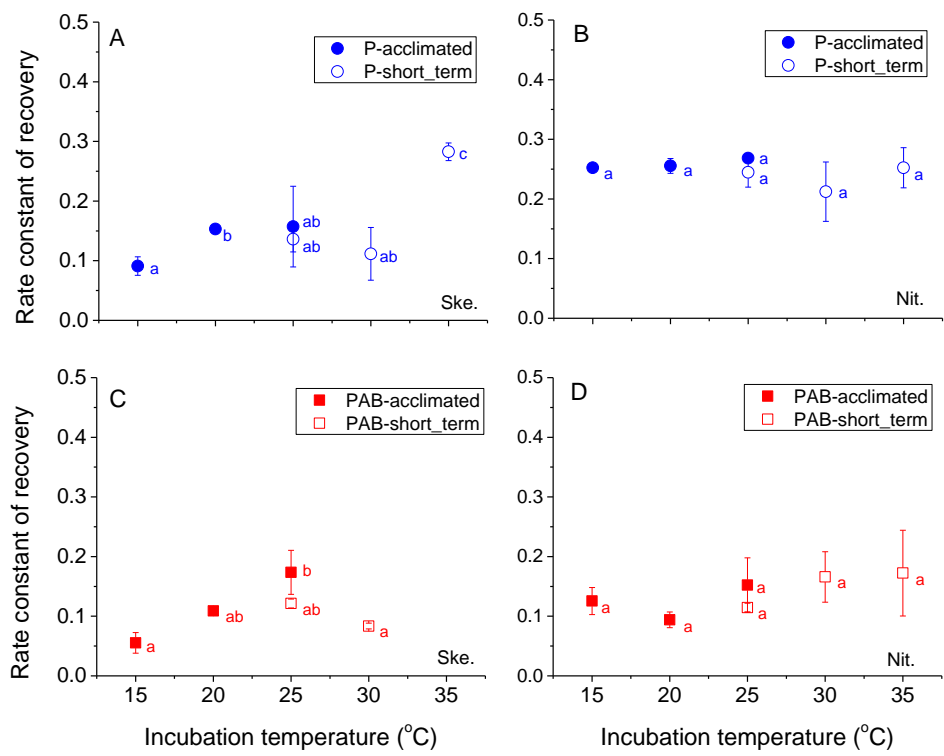
576  
 577  
 578  
 579  
 580  
 581  
 582  
 583

Fig 5



584  
585  
586  
587  
588  
589  
590  
591

Fig 6



593

594 Fig 7

595

596